CONF-900403--1

DE90 002708

CONF-900403--1

EVALUATION OF RADIATION-INDUCED SENSITIZATION USING ELECTROCHEMICAL POTENTIOKINETIC REACTIVATION TECHNIQUE FOR AUSTENITIC STAINLESS STEELS*

T. Inazumi
Japan Atomic Energy Research Institute, Tokai-mura, Ibaraki-ken, 319-11, Japan
(assigned to Oak Ridge National Laboratory, P.O. Box 2008, Oak Ridge, TN 37831-6376)

G.E.C. Bell
Oak Ridge Associated Universities, P.O. Box 2008, Oak Ridge, TN 37831-6156

A. Hishinuma
Japan Atomic Energy Research Institute

ABSTRACT

The electrochemical potentiokinetic reactivation (EPR) test technique was applied to the determination of sensitization in a neutron-irradiated (420°C, 10 dpa) titanium-modified austenitic stainless steel. Miniaturized specimens (3 mm diam by 0.25 mm thick) in solution-annealed and 25% cold-worked conditions were tested. The degree of sensitization (DOS) was calculated in terms of the reactivation charge (Pa). Results indicated the occurrence of radiation-induced sensitization when compared to control specimens thermally aged at the irradiation temperature. Post-EPR examination of the specimen surfaces showed etching across the face of each grain as well as at grain boundaries. This indicates that the Pa value normalized by the total grain boundary area, which is an accepted EPR-DOS criterion, cannot be directly used as an indicator of the DOS to determine the susceptibility of this irradiated material to intergranular stress corrosion cracking (IGSCC). Further investigations are necessary to correlate the results in this study to the IGSCC susceptibility of the irradiated stainless steel.

KEY WORDS: Stress corrosion cracking, sensitization, austenitic stainless steel, electrochemical measurement, fusion reactor, neutron irradiation, radiation-induced segregation.

---

*Research sponsored by the Office of Fusion Energy, U.S. Department of Energy, under contract DE-AC05-84OR21400 with the Martin Marietta Energy Systems, Inc., and the Japan Atomic Energy Research Institute.

MASTER

INTRODUCTION

Irradiation-assisted stress corrosion cracking (IASCC) is considered one of the major environmental degradation mechanisms of austenitic stainless steels in water-cooled nuclear power systems.[1-3] IASCC has been observed in type 304 stainless steel which was exposed to fast neutron (E > 1 MeV) fluence greater than ~5 × 10^{20} n/cm^2 and has been manifested in the form of intergranular stress corrosion cracking (IGSCC).[1] It has been suggested that changes in grain boundary composition caused by radiation-induced segregation (RIS) played an important role in increasing the IASCC susceptibility of stainless steels.[3-15] Chromium depletion from grain boundaries is one of the major phenomena caused by RIS[4,10-14] and has been suggested as a contributor to IASCC.[13-15] The chromium concentration at grain boundaries can be reduced by RIS to below 12 wt %, the minimum chromium level required to form a protective film on austenitic steel surfaces.[11,12] In the case of water-cooled stainless steel components for fusion reactors, IASCC will also be a degradation mechanism.[16,17] In this case, RIS characteristics of materials may be different from those in light-water reactors because of the harder neutron spectrum and higher neutron flux (viz., higher damage rate and helium production).[18]

An electrochemical characterization system was developed to evaluate the degree of sensitization associated with chromium depletion along grain boundaries in neutron-irradiated austenitic stainless steels.[19] The system was designed to use miniaturized disk-type specimens, 3 mm diam by 0.25 mm thick, because of limited space for specimens in irradiation facilities, the need for low radiation exposure of personnel who handle specimens and do testing, and its ease of use for TEM analysis. Since the electrochemical testing is nondestructive, the microstructural analysis can then be conducted on the same specimen following the testing and, thus, electrochemical properties can be directly related to microstructures. Thermally induced sensitization in titanium-modified austenitic stainless steel specimens of this geometry was successfully detected using the electrochemical potentiokinetic reactivation (EPR) technique.[19] In the present study, the EPR technique was applied to the evaluation of radiation-induced sensitization in a candidate austenitic stainless steel, PCA, designed for use in fusion reactors.

EXPERIMENTAL PROCEDURES

The material used in this study was a titanium-modified austenitic stainless steel developed by the U.S. Fusion program, designated as PCA. The chemical composition of the steel is shown in Table 1. Disk specimens, 3 mm in diameter, were punched from 0.25-mm-thick sheet of the material and solution annealed at 1100°C for 30 min. Specimens in the 25% cold-worked condition were also prepared.

The specimens were irradiated in the Materials Open Test Assembly (MOTA) of the Fast Flux Test Facility (FFTF) in Hanford, Washington, at a temperature of 420°C to a level of 10 displacements per atom (dpa). Control specimens were thermally aged at 420°C for 5000 h and then water quenched to simulate the thermal history of the irradiated specimens.

The EPR testing system consists of the electrochemical characterization apparatus and the surface preparation equipment designed for handling radioactive specimens and waste. A detailed description of the testing system was given elsewhere.[19] Prior to the EPR test, specimens were electropolished with a vertical jet-type polishing apparatus to remove surface oxide films and to obtain smooth surfaces without grain boundary etching so as to obtain the maximum electrochemical sensitivity.[19] Single loop EPR tests were performed following the test conditions recommended by

W. L. Clarke et al.[20] A summary of the test conditions is given in Table 2. The degree of sensitization (DOS) was determined by calculating the normalized reactivation charge (Pa).[20]

Observation of the specimen surfaces after EPR testing was accomplished with an optical microscope and a scanning electron microscope (SEM).

RESULTS

EPR Test

Reactivation curves of the irradiated and thermally aged control specimens are shown in Figure 1. The reactivation current density peak appeared at approximately −120 mV vs SCE for all the specimens. However, the peak current densities for the irradiated specimens were approximately two-orders-of-magnitude higher than those of the thermally aged specimens for both the solution annealed and cold worked conditions. There was only a slight difference between the reactivation curves for the solution annealed and the cold worked conditions. The Flade potential – that is, the potential at which the current started increasing – was substantially higher for the irradiated specimens (by approximately 75 and 125 mV for the annealed and the cold worked conditions, respectively).

The normalized reactivation charge [(Pa) (coulombs/cm^2)] was calculated for each specimen and the results are shown in Table 3. The Pa values of the irradiated specimens were two orders-of-magnitude higher than those of the thermally aged control specimens for both the solution annealed and cold worked conditions. There was no significant difference in the Pa value between the solution annealed and cold worked conditions. The Pa values of two specimens in each condition were in good agreement.

Surface Examination

Optical micrographs of the specimen surfaces after EPR testing are shown in Figures 2 and 3. The thermally aged specimens did not show etching in either the annealed or the cold-worked condition [Figures 2(a) and 3(a)]. On the other hand, the irradiated specimens were apparently etched in both conditions [Figures 2(b) and 3(b)]. For the irradiated annealed PCA, the grain boundaries appeared to be weakly etched and the grain faces also had a very finely etched structure [Figure 2(b)]. The cold-worked PCA showed similarly etched grain boundaries and etched slip lines [Figure 3(b)].

SEM micrographs of the specimen surface of the irradiated annealed PCA are shown in Figure 4. The grain boundary etching was discontinuous and the width of the etching was not uniform [Figure 4(a)]. The finely etched structure observed over the grain faces [Figures 2(b) and 3(b)] resulted from corrosion-induced dimpling with an average dimple diameter of 0.5 μm [Figure 4(b)]. The depth of etching associated with dimpling was much less than the depth at the grain boundaries. The width of the etched grain boundaries was approximately 1 μm at the widest portion, and it narrowed to less than 100 nm near the botton [Figure 4(c)]. A SEM micrograph of the irradiated cold-worked PCA is shown in Figure 5. The grain boundary etching was similar to that of the irradiated annealed specimen. Dimpling over grain faces was also observed.

DISCUSSION

Microstructural observations revealed that the grain boundaries of irradiated PCAs were apparently etched after EPR testing. This indicates that sensitization

associated with chromium depletion along grain boundaries was induced by the neutron irradiation, as previously reported by Taylor for 20Cr-25Ni-Nb stabilized steel irradiated up to 5.5 dpa at 350 to 520°C.[15] This also suggests that radiation-induced sensitization was detectable by the EPR test technique in the same manner as thermally induced sensitization.[19] The narrow width of the etched grain boundaries indicates that RIS, which has been reported to be effective over distance less than 100 nm (refs. 11,12), is one of the possible mechanisms for the sensitization.

The reactivation charge [Pa (time integral of current density)] is conventionally used as a criterion to determine the DOS. Good correlation between intergranular stress corrosion cracking (IGSCC) susceptibility of austenitic stainless steels (type 304) and the Pa value has been demonstrated.[20-22] The Pa value is generally normalized to represent the charge per unit grain boundary area under the assumption that most of the reactivation current comes from the grain boundaries.[20-22] It has been suggested that IGSCC can occur when the Pa value exceeds about 2 coulombs/cm^2 for type 304 stainless steels.[21] The Pa values of irradiated PCAs (Table 3) are an order-of-magnitude higher than this critical value. However, as shown in Figures 2(b) and 3(b), both the grain boundaries and the grain faces were etched during the reactivation process. Since the grain faces apparently contribute to reactivation current, the normalized Pa value per unit grain boundary area overestimates the actual reactivation charge associated with the grain boundaries.

If it is assumed that the reactivation current is uniformly distributed between the grain boundaries and faces, the Pa value can be normalized to represent the charge per unit grain boundary area using the total tested area of the specimens instead of only that of the grain boundaries. The results of these calculations are shown in Table 4. These Pa values possibly underestimate the contribution from the grain boundaries based on the relative deep etching at the grain boundaries as compared to the dimples in the grain faces. Nevertheless, the Pa values of the irradiated specimens are still an order-of-magnitude higher than those of the thermally aged specimens and close to 2 coulombs/cm^2, the critical value for the susceptibility of type 304 stainless steels to IGSCC. For molybdenum-containing austenitic stainless steels (e.g., type 316), reported Pa values were lower than for type 304 for the same degree of thermally induced sensitization (as determined by the Strauss test[23]). Therefore, a lower critical value of Pa, as compared to type 304, may be required for molybdenum-containing austenitic stainless steels to be susceptible to IGSCC. We suggest that the neutron irradiation at 420°C up to 10 dpa could have increased the DOS of PCA to the level at which IASCC could occur. However, radiation induced sensitization and thermally induced sensitization are substantially different processes, and direct application of the EPR-DOS criterion for thermally sensitized materials is not valid. The post-EPR microstructure shown by the irradiated specimens apparently differs from that of thermally sensitized specimens with similar Pa values (an example is shown in Figure 6). For the irradiated specimens, grain boundary etching was narrower. Therefore, smaller initial flaw size may exist for the irradiated material. Changes in the mechanical properties by the irradiation (e.g., matrix hardening and decrease in ductility[24-26]) may also affect the susceptibility of the irradiated PCA to IGSCC. Further investigations, including stress corrosion cracking tests on the same irradiated materials, are necessary to correlate the EPR test results of this study to the IGSCC susceptibility.

Figure 7 shows an optical micrograph of irradiated PCA after EPR testing was interrupted half-way to the peak current density. The initiation of fine etching was observed. The dimple-shape etching of the grain faces apparently results from the continuing increase in density of this fine etching. Under the irradiation condition used in this study, small-scale voids (10–20 nm in diameter) were formed in the grain interiors.[27] It has been demonstrated that, under irradiation, chromium

depletion can occur at microscopic free surfaces in grain interiors (e.g., voids) as well as at grain boundaries[28]. Therefore, the dimple-shaped etching on grain faces could be caused by RIS of chromium away from voids.

CONCLUSIONS

Radiation-induced sensitization of the neutron-irradiated titanium-modified austenitic stainless steel was evaluated by the EPR test technique using miniaturized specimens. The following conclusions were obtained:

1. Significant changes in electrochemical properties of titanium-modified austenitic stainless steel due to irradiation at 420°C up to 10 dpa were detected by the miniaturized EPR test technique.

2. EPR test results and resulting grain boundary etching indicated the occurrence of radiation-induced sensitization.

3. In addition to grain boundaries, grain faces showed shallow dimple-shaped etching after EPR testing. Therefore, the reactivation charge normalized by total grain boundary area, which is an accepted EPR-DOS criterion for the IGSCC susceptibility of thermally sensitized stainless steels, was not directly applicable to radiation-induced sensitization for the condition investigated.

4. For this irradiation condition, 25% cold work did not have significant effects on the EPR test results.

5. Further investigations are necessary to correlate the results in this study to the IGSCC susceptibility of the irradiated stainless steel.

REFERENCES

1. A. J. Jacobs, G. P. Wozadlo, Proc. of International Conference on Nuclear Power Plant Aging, Availability Factor and Reliability Analysis, ASM, pp. 173–80, 1985.

2. W. L. Clarke, A. J. Jacobs, Materials in Nuclear Energy, (Proc. of Int. Conf.), ASM, pp. 153–60, 1982.

3. R. N. Duncan, Stainless Steel Failure Investigation Program, Final Summary Report, GEAP-5530, 1968.

4. K. Fukuya, S. Nakahigashi, S. Ozaki, M. Terasawa, S. Shima, Proc. of the Third International Symposium on Environmental Degradation of Materials in Nuclear Power System-Water Reactors, TMS, pp. 665–71, 1987.

5. A. J. Jacobs, G. P. Wozadlo, N. Nakata, T. Yoshida, I. Masaoka, Proc. of the Third International Symposium on Environmental Degradation of Materials in Nuclear Power System-Water Reactors, TMS, pp. 673–81, 1987.

6. E. P. Simonen, R. H. Jones, Proc. of the Third International Symposium on Environmental Degradation of Materials in Nuclear Power System-Water Reactors, TMS, pp. 683–90, 1987.

7. H. Hanninen, Aho-Mantila, Proc. of the Third International Symposium on Environmental Degradation of Materials in Nuclear Power System-Water Reactors, TMS, pp. 77–92, 1987.

8. F. Garzarolli, D. Alter, P. Dewes, J. L. Nelson, Proc. of the Third International Symposium on Environmental Degradation of Materials in Nuclear Power System-Water Reactors, TMS, pp. 657–64, 1987.

9. Aho-Mantila, H. Hänninen, Materials for Nuclear Reactor Core Applications (Proc. of Int. Conf.), Vol. 1, BNES, pp. 349–56, 1987.

10. E. A. Kenik, Proc. of Mat. Res. Soc. Symp., Vol. 62, pp. 209–16, 1986.

11. D.I.R. Norris, C. Baker, J. M. Titchmarsh, Radiation-Induced Sensitization of Stainless Steels (Proc. of the Symposium held at Berkeley Nuclear Laboratories, 23 September 1986), CEGB, pp. 86–98, 1987.

12. J. M. Perks, A. D. Marwick, C. A. English, Radiation-Induced Sensitization of Stainless Steels (Proc. of the Symposium held at Berkeley Nuclear Laboratories, 23 September 1986), CEGB, pp. 15–34, 1987.

13. A. J. Jacobs, R. E. Clausing, L. Heatherly, R. M. Kruger, Irradiation-Assisted Stress Corrosion Cracking and Grain Boundary Segregation in Heat Treated Type 304SS, CONF-880613-3, 1988.

14. P. L. Andresen, F. P. Ford, S. Murphy, J. Perks, Proc. of the Fourth International Symposium on Environmental Degradation of Materials in Nuclear Power System-Water Reactors (to be published).

15. C. Taylor, Radiation-Induced Sensitization of Stainless Steels (Proc. of the Symposium held at Berkeley Nuclear Laboratories, 23 September 1986), CEGB, pp. 60–73, 1987.

16. C. C. Baker, Fusion Technology, Vol. 15, pp. 849–57, 1989.

17. R. H. Jones, Fusion Reactor Materials (Semiannual Progress Report, March 31, 1988), DOE/ER-0313/4, pp. 184–88, 1988.

18. S. Ohnuki, H. Takahashi, R. Nagasaki, J. Nucl. Mater., Vol. 155–157, pp. 823–27, 1988.

19. T. Inazumi, G.E.C. Bell, K. Kiuchi, J. Nucl. Mater. (ICFRM-4) (to be published).

20. W. L. Clarke, R. L. Cowan, W. L. Walker, Intergranular Corrosion of Stainless Alloys, ASTM STP 656, pp. 99–132, 1978.

21. W. L. Clarke, V. M. Romero, J. C. Danko, Detection of Sensitization in Stainless Steel Using Electrochemical Techniques, GEAP-21382, 1976.

22. A. J. Giannuzzi, Studies on AISI Type 304 Stainless Steel Piping Weldments for Use in BWR Application, EPRI NP-944, 1978.

23. F. Umemura, T. Kawamoto, Boshoku Gijutsu, Vol. 28, pp. 24–31, 1979.

24. P. J. Maziasz, D. N. Braski, J. Nucl. Mater. Vol. 141–143, pp. 973–77, 1986.

25. M. P. Tanaka, S. Hamada, A. Hishinuma, M. L. Grossbeck, J. Nucl. Mater. Vol. 155-157, pp. 957–62, 1988.

26. M. L. Grossbeck, Fusion Reactor Materials (Semiannual Progress Report, September 30, 1989), DOE/ER-0313/7 (to be published).

27. R. E. Stoller, P. J. Maziasz, A. F. Rowcliffe, M. P. Tanaka, J. Nucl. Mater. Vol. 155-157, pp. 1328–34, 1988.

28. C. M. Shepherd, T. M. Williams, Proc. of the Fourth International Symposium on Environmental Degradation of Materials in Nuclear Power System-Water Reactors (to be published).

TABLE 1
CHEMICAL COMPOSITION OF PCA (wt %)

C	Si	Mn	P	S	Ni	Cr	Mo	Ti	Fe
0.05	0.4	1.8	0.01	0.003	16.2	14.0	2.3	0.24	bal

TABLE 2
EPR TEST CONDITIONS

Solution	0.5 M H_2SO_4 + 0.01 M KSCN
Temperature, °C	30
Passivation	2 min at +200 mV vs SCE
Reactivation scan, V/h	6

TABLE 3
REACTIVATION CHARGE VALUE
(NORMALIZED BY TOTAL GRAIN BOUNDARY AREA)

Steel		Pa, coulombs/cm²	
		Aged*	Irradiated
PCA	Solution Annealed	0.14	64.1 59.9
PCA	25% Cold Worked	0.24	53.0 54.0

*Average value of two specimens aged at 420°C for 5000 h.

TABLE 4
REACTIVATION CHARGE VALUE
(CALCULATED USING TOTAL TESTED AREA)

Steel		Pa, coulombs/cm²
PCA	Solution Annealed	1.85 1.73
PCA	25% Cold Worked	1.53 1.56

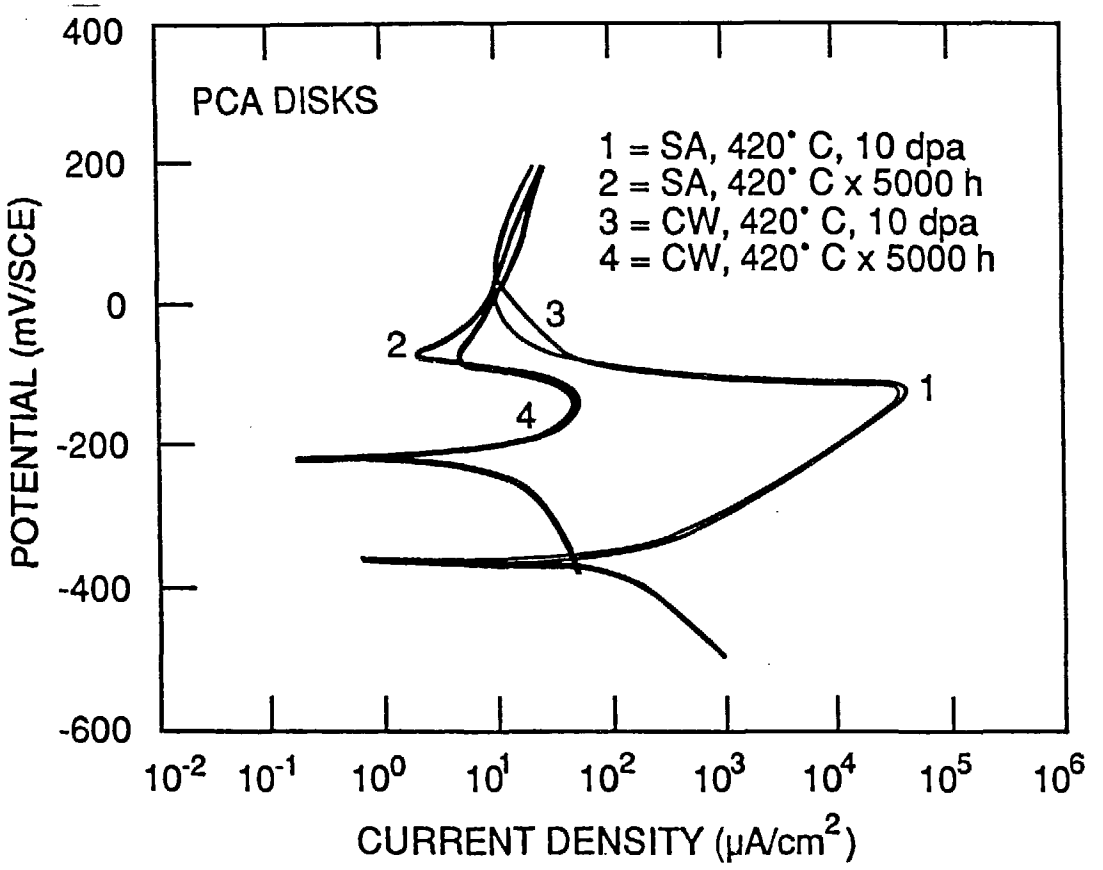

FIGURE 1 - Reactivation curves of PCA.

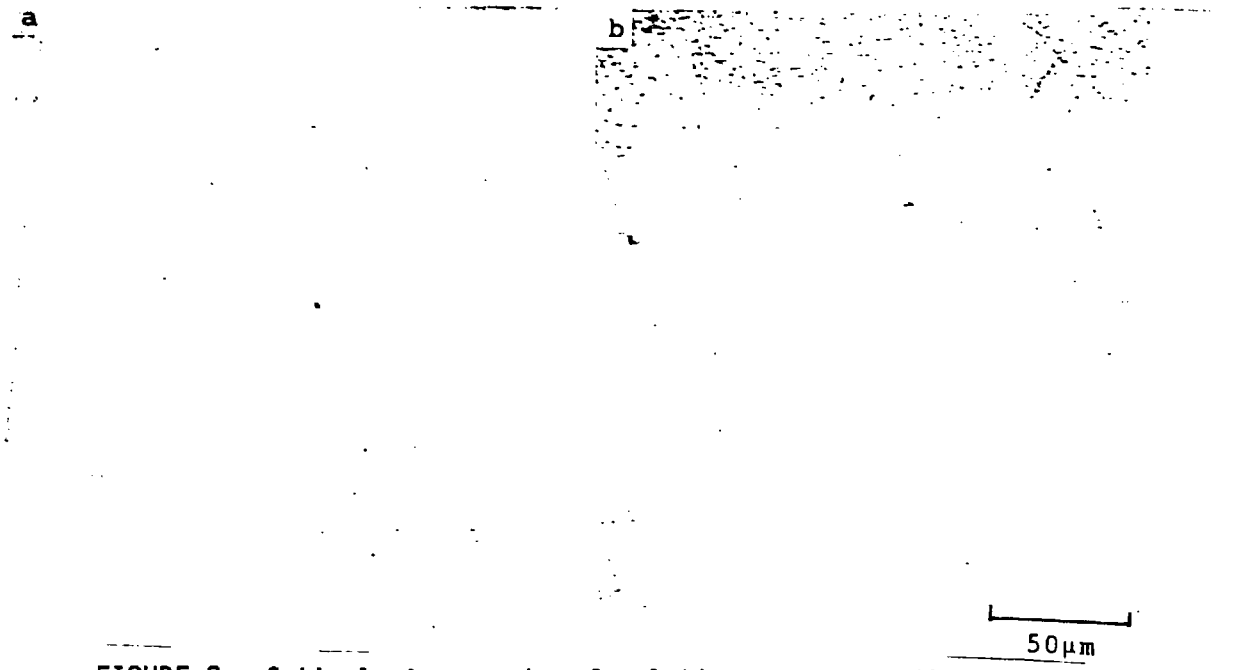

FIGURE 2 - Optical micrographs of solution annealed PCA after EPR tests. (a) Thermally aged, (b) neutron irradiated.

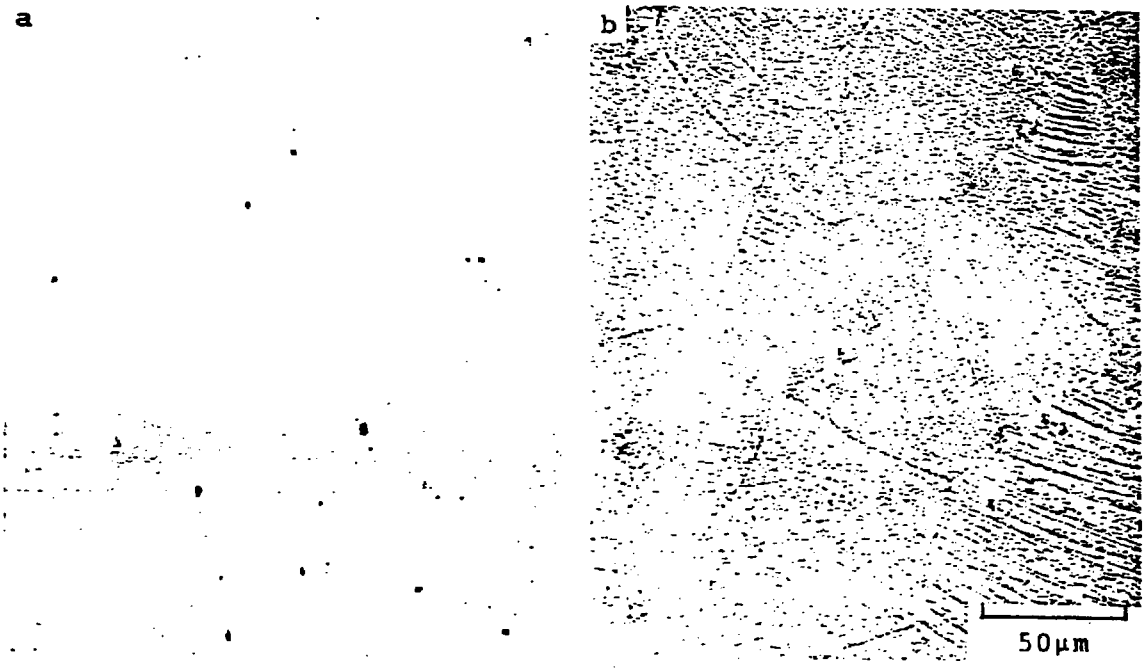

FIGURE 3 - Optical micrographs of 25% cold-worked PCA after EPR tests. (a) Thermally aged, (b) neutron irradiated.

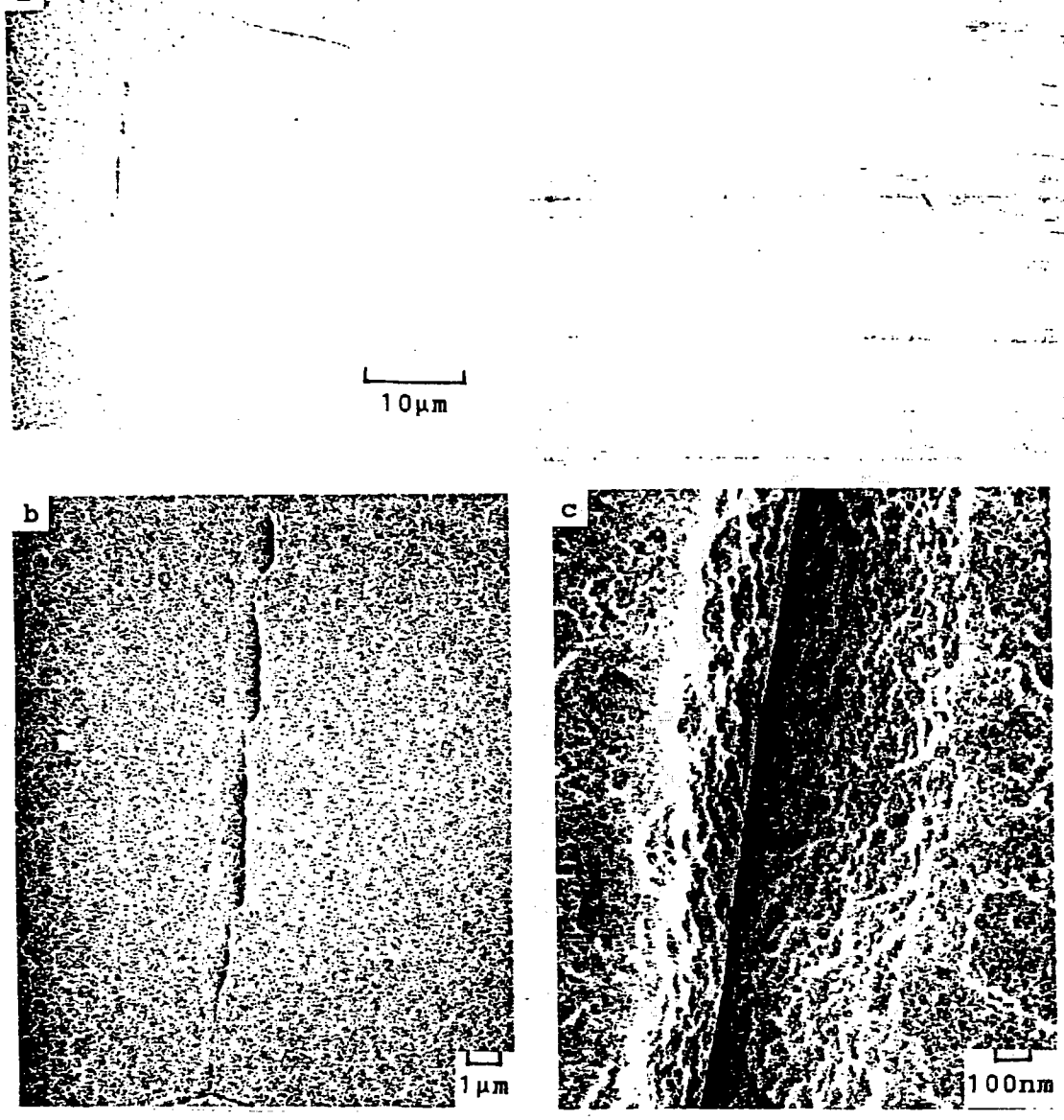

FIGURE 4 - SEM micrographs of irradiated annealed PCA after EPR test.

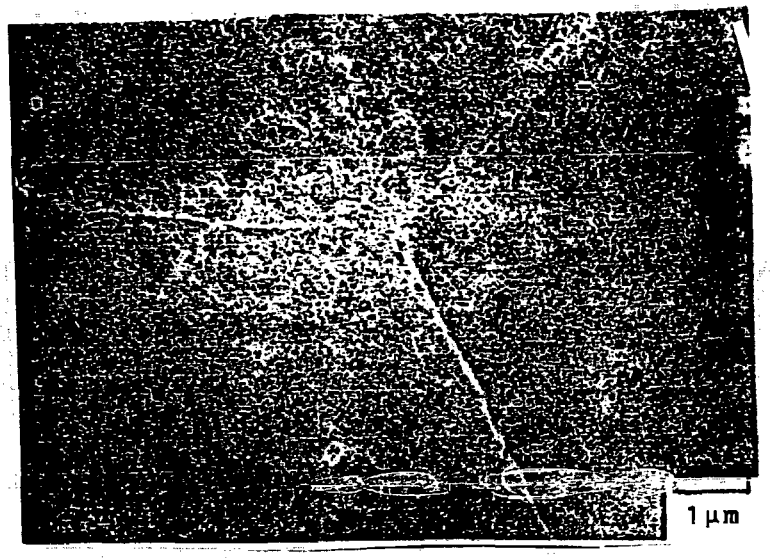

FIGURE 5 - SEM micrograph of irradiated 25% cold-worked PCA after EPR test.

FIGURE 6 - Optical micrograph of thermally sensitized annealed PCA after EPR test (Pa = 1.64 coulombs/cm^2).

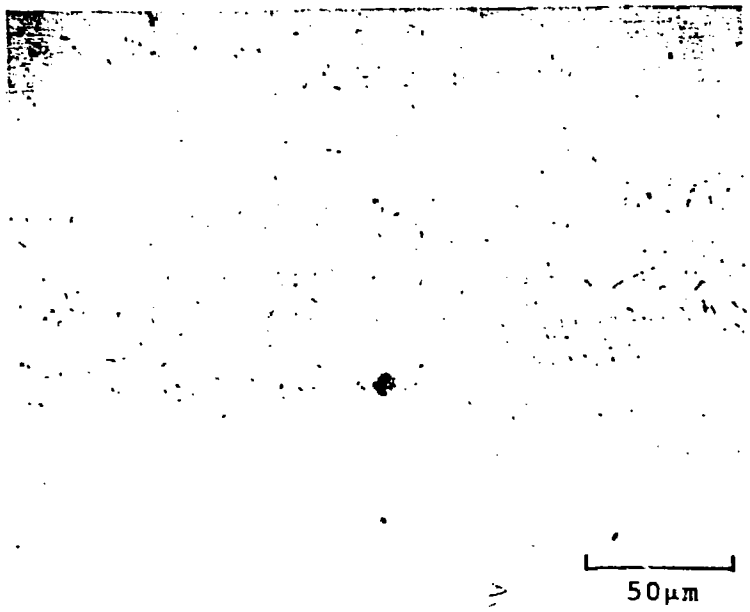

FIGURE 7 - Optical micrograph of irradiated annealed PCA after EPR test - interrupted half-way to the peak current.

FIGURES

FIGURE 1 - Reactivation curves of PCA.

FIGURE 2 - Optical micrographs of solution annealed PCA after EPR tests. (a) Thermally aged, (b) neutron irradiated.

FIGURE 3 - Optical micrographs of 25% cold-worked PCA after EPR tests. (a) Thermally aged, (b) neutron irradiated.

FIGURE 4 - SEM micrographs of irradiated annealed PCA after EPR test.

FIGURE 5 - SEM micrograph of irradiated 25% cold-worked PCA after EPR test.

FIGURE 6 - Optical micrograph of thermally sensitized annealed PCA after EPR test (Pa = 1.64 coulombs/cm^2).

FIGURE 7 - Optical micrograph of irradiated annealed PCA after EPR test - interrupted half-way to the peak current.